The values are

$$R_{Of} = 9{\cdot}14 \times 10^{-9}(1 + \cos\beta)$$
$$R_{Hf} = 7{\cdot}96 \times 10^{-9} + 6{\cdot}99 \times 10^{-9}\cos\beta - 3{\cdot}89 \times 10^{-12}\sin\beta$$
$$R^{L}_{H\,II} = 1{\cdot}52 \times 10^{-7}.$$

The fringe pattern is essentially the same as for the 220 reflection, except that the intensities are much weaker.

In conclusion, we have shown how the fringe pattern and all relevant intensities for a LLL interferometer can be obtained by repeated applications of the expressions for the amplitudes obtained for diffraction through a single slab. The neutron and the X-ray cases can both be treated with the same formalism, provided the appropriate parameters are introduced. The treatment is given in terms of plane waves, which is appropriate if global integrated intensities (*i.e.* counting rates) are of interest, rather than spatial intensity distributions across the beams emerging from the last crystal of the interferometer.

This work was supported by the National Science Foundation, Grant DMR-8715503.

References

BATTERMAN, B. W. & COLE, H. (1964). *Rev. Mod. Phys.* **36**, 681-717.
BAUSPIESS, W., BONSE, U. & GRAEFF, W. (1976). *J. Appl. Cryst.* **9**, 68-80.
BONSE, U. & HART, M. (1965). *Z. Phys.* **188**, 154-164.
BONSE, U. & TE KAAT, E. (1971). *Z. Phys.* **243**, 14-45.
KATO, N. (1968). *J. Appl. Phys.* **39**, 2231-2237.
JAMES, R. W. (1962). *The Optical Principles of the Diffraction of X-rays*, p. 70. Ithaca: Cornell Univ. Press.
PETRASCHECK, D. (1979). *Neutron Interferometry*. Proceedings of an International Workshop held 5-7 June 1978 at the Institut Max von Laue-Paul Langevin, Grenoble, edited by U. BONSE & H. RAUCH, pp. 108-134. Oxford: Clarendon Press.
RAUCH, H. & SUDA, M. (1974). *Phys. Status Solidi A*, **25**, 495-505.
RAUCH, H., TREIMER, W. & BONSE, U. (1974). *Phys. Lett. A*, **47**, 369-371.
STAUDENMANN, J. L., WERNER, S. A., COLELLA, R. & OVERHAUSER, A. W. (1980). *Phys. Rev.* **21**, 1419-1438.
ZACHARIASEN, W. H. (1945). *Theory of X-ray Diffraction in Crystals*, inc. Sect. III. New York: John Wiley.

Acta Cryst. (1988). A**44**, 1059-1065

X-ray Powder Diffraction of Anthracene at Hydrostatic Pressures up to 0·9 GPa

BY R. PUFALL AND J. KALUS

Experimentalphysik I der Universität Bayreuth, Postfach 101252, *D*-8580 *Bayreuth, Federal Republic of Germany*

(*Received* 3 *February* 1988; *accepted* 22 *June* 1988)

Abstract

An X-ray powder diffraction cell for pressures up to 0·9 GPa was constructed. The pressure dependence of the unit-cell parameters and pressure-induced changes of the orientation of anthracene molecules were determined at ambient temperature. The diffraction patterns were analysed with a modified Rietveld program. The comparison with calculations based on atom-atom potentials (6-exp-type) between rigid molecules using Williams's [*J. Chem. Phys.* (1967). **47**, 4680-4684] and Kitaigorodski's [*J. Chim. Phys. Phys. Chim. Biol.* (1966). **63**, 9-16] parameters shows that satisfactory agreement can be obtained with the predictions.

I. Introduction

Anthracene crystallizes in space group $P2_1/a$ (C^5_{2h}) with two molecules in the unit cell. There is no phase change at room temperature at the pressures used in our experiment.

The crystalline structure of anthracene is mainly determined by weak van der Waals-like forces, whereas the binding within the molecule is provided by strong covalent bonds. For this reason the planar shape of the molecule remains essentially unchanged when it is incorporated into a crystal lattice. The distances between the molecules are changed under pressure. Therefore it is possible to probe the shape of intermolecular forces or potentials. It turns out that, apart from distances, the orientations of molecules are altered too. Both effects can be seen in elastic scattering *via* accurate determination of Bragg intensities as a function of pressure. This method is in a way complementary to inelastic neutron scattering where information about the intermolecular forces can be deduced from measured phonon dispersion curves. The advantage of inelastic neutron scattering experiments stems from the fact that more experimental data are available to fit a model.

In the next sections we report the experimental details, the results of the powder diffraction

0108-7673/88/061059-07$03.00

experiments with pressures up to nearly 0·9 GPa together with the data refinement procedures. We present a comparison between experimental results and data calculated *via* an atom-atom potential between the molecules. The same potential was used for an evaluation of anthracene phonon dispersion curves by Dorner *et al.* (1982).

II. Experiment

The experimental set up consisted of a conventional powder diffractometer using Mo $K\alpha_1$ radiation, Si monochromator, scintillation counters and counting electronics.

The diffractometer, data collection and processing were controlled by a microcomputer in combination with a fast computer. The temperature variation of the whole diffractometer was kept below ±0·2 K. A thin plastic foil introduced into the path of the incoming beam scattered some fraction of the X-ray beam in the direction of a monitor counter. This signal was used to correct the scattered X-ray intensities. For an effective increase of the number of crystallites the pressure cell oscillated at angles ranging from 0 to 5°, with the same number of oscillations for each scattering angle.

Commercial 'anthracene for scintillation measurements' with a purity exceeding 99% (Merck) was used. The raw material was ground and sieved to a particle size smaller than 20 μm at the temperature of solid CO_2. Fine sieving was possible at this temperature. The pressure cell itself weighs about 10 kg and is easy to handle on a commercial goniometer. the maximum pressure that can be used safely is about 0·9 GPa. Pressure is provided by means of helium; therefore purely hydrostatic pressure is guaranteed and any background scattering from the pressure-transmitting medium is minimized. The window for the X-rays is made from a cylindrical piece of boron carbide with an outer diameter of 20·3 mm and an overall length of 40 mm. The powder sample filled the 5 mm bore of the cylinder. Boron carbide is brittle and shows a tensile strength of the order of only 0·1 GPa. Therefore a massive steel jacket with a window 4 mm in height for the X-rays was constructed to transmit a preload of the order of 1 GPa to the boron carbide. A more detailed discussion of the pressure-cell design will be given in a future paper. The overall design resembles the pressure cell constructed for neutron scattering experiments by Bloch, Paureau, Voiron & Parisot (1976). The absorption of Mo $K\alpha$ X-rays amounts to approximately 80%. Usable scattering angles are nearly up to 360°, the sample volume and the beam height being 79 mm^3 and 4 mm respectively. By means of well collimated X-ray beams it was possible to record high-quality powder diffraction patterns without any noticeable background scattering from the pressure cell itself.

III. Results and data evaluation

For pressures up to 0·85 GPa several series of measurements were performed. Examples of diffraction patterns at 0 and 0·85 GPa are shown in Fig. 1. A shift of the peaks and a change of intensity is observed which can be very different for the individual reflections.

The structure of anthracene at normal pressure (Mason, 1964) served as input data for a refinement with a modified Rietveld program (Wiles & Young, 1981). The aim of this method (Rietveld, 1967) is to produce refined parameter values from powder diffraction data. The quantity minimized, called the residual, R, is

$$R = \sum_i w_i (Y_i - Y_{bi} - Y_{ci})^2. \qquad (1)$$

The summation is over all the steps i in the pattern. $w_i = 1/(Y_i + Y_{bi})$ is the weight, whereas Y_i, Y_{bi} and Y_{ci} are the measured intensity, the background intensity and the calculated intensity at the ith step.

The calculation of Y_{ci} was performed in the following way:

$$Y_{ci} = c \sum_K L_K |F_K|^2 \Phi(2\theta_i - 2\theta_K - \delta) P_K A_i \qquad (2)$$

where $K = (h, k, l)$ with h, k and l being used to denote the reflections (with related Bragg angle θ_K) that contribute to the intensity at the angle θ_i of the diffraction pattern. c is a scale factor, F_K is the structure factor, and L_K is the Lorentz, polarization and multiplicity factor for the Kth Bragg reflection. P_K, A_i, Φ and δ are the orientation function for uniaxial texture, the absorption and area factor, the normalized reflection profile function and the offset of the zero point of the diffraction pattern respectively.

The well collimated incoming beam illuminates only part of the powder sample and by means of some slits only a certain part of the sample is seen by the detector. Both factors give a change of sensitive volume depending strongly on scattering angle. Therefore the absorption and area factor A_i changed substantially with scattering angle $2\theta_i$. A_i was calculated with the sample size and the collimations taken into account. By means of the strong collimation no scattering from the walls was seen by the detector, which guaranteed a very low background. In the Rietveld program (Wiles & Young, 1981) we implemented the following modifications:

(1) The anthracene molecules were assumed to be rigid. We allowed rearrangement of orientation with pressure, described by three Eulerian angles ψ, φ and θ.

(2) The anisotropic temperature factor according to the model for rigid molecules was represented by a translation and a libration tensor (Cruickshank, 1956).

(3) A pressure dependence of the anisotropic temperature factor was taken into account, described by a Grüneisen parameter (Alt & Kalus, 1982).

(4) A systematic shift of the position of the diffraction maxima due to the finite solid angles of the powder diffractometer was taken into account.

(5) A new profile function which reproduced well the angle-dependent shape of the diffraction profiles was introduced.

We described the orientation of the molecules in an orthonormal (x, y, z) system with x axis parallel to the a axis, y axis parallel to the b axis and z axis perpendicular to the ab plane of the unit cell. Fixed to the molecules was a further orthonormal (x', y', z') system, the axes of which were parallel to the axes of the inertia tensor of the molecules. The (x', y', z') system and the shape of the molecule are shown in Fig. 2.

For the calculation of the structure factor we took into account the Debye-Waller factor as mentioned above. Cruickshank (1956) showed that a translation (T_{ij}) and a libration (L_{ij}) tensor are sufficient to describe the Debye-Waller factor for a rigid molecule with a centre of symmetry. At normal pressure we used the known tensors T_{ij} and L_{ij} from Pawley (1967). To take into account the pressure dependence of the tensor elements several approximations were made and the volume dependence of normal-mode frequencies ω were described by means of Grüneisen-mode parameters

$$\gamma(\mathbf{q}, s) = -[V/\omega(\mathbf{q}, s)]\partial\omega(\mathbf{q}, s)/\partial V \qquad (3)$$

where V, $\mathbf{q}$ and s are the crystal volume, phonon wave vector and branch index respectively. For lattice modes experimental values of $\gamma(\mathbf{q}, s)$ are available for some Raman active modes at $\mathbf{q}=0$ (Häfner & Kiefer, 1987). The values lie between $\gamma=2{\cdot}92$ and $4{\cdot}39$ for modes below $118\ \mathrm{cm}^{-1}$. The values tend to increase for smaller ω values. It is known that γ values for $\mathbf{q}\neq 0$ are not very different from γ values at $\mathbf{q}=0$ (Schmelzer *et al.*, 1981). Instead of the individual $\gamma(\mathbf{q}, s)$ values we introduced a mean Grüneisen parameter $\bar{\gamma}$, which was used as a fit parameter for the data and turned out to be $3{\cdot}31$. Under these approximations it is found that the pressure dependence of $T_{ij}(p)$ (Alt & Kalus, 1982) is

$$T_{ij}(p) = T_{ij}(0)\{1 - \bar{\gamma}[V(p) - V(0)]/V(0)\}^{-2}. \qquad (4)$$

A similar expression is obtained for $L_{ij}(p)$.

It was observed that a weak (001) texture was present in our powder samples. This had to be corrected with a parameter P for uniaxial orientation. For good fits the profile function Φ must be known. First tests showed that neither Gaussian, Lorentzian nor modified Lorentzian functions give good fits. It was found that for our experimental situation the

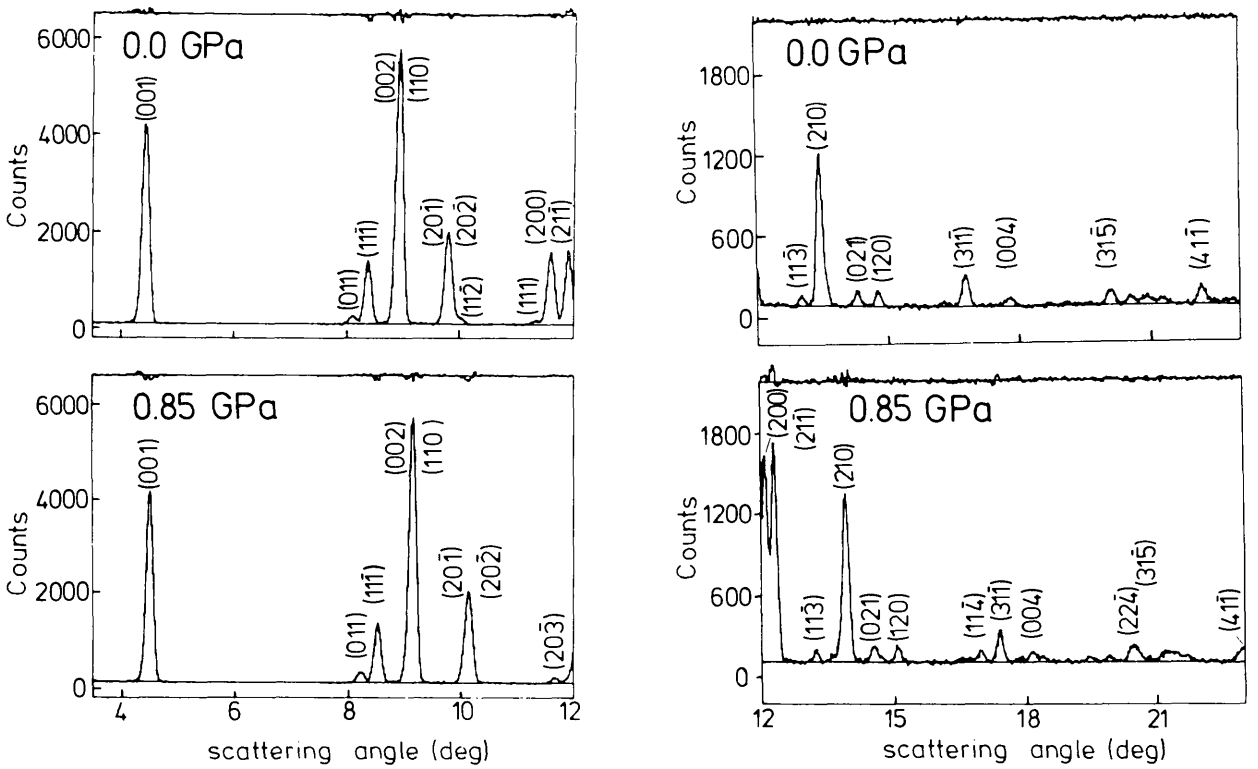

Fig. 1. The measured diffraction pattern at 0·0 (upper curves) and 0·85 GPa (lower curves). The differences between measured and fitted intensities are shown at the top of the figures. The background is also shown as a solid line.

modified and properly normalized Gaussian function shown below leads to satisfactory results:

$$\Phi(x) = A \exp\left[-(\ln 2)|2x/H_w|^n\right] \qquad (5)$$

with $x = 2\theta - 2\theta_K - \delta + G(2\theta_K)$. H_w is the full width at half maximum. The exponent n was expressed by a linear function of the scattering angle 2θ. By computer simulations of individual X-ray beams it was found that a systematic shift of Bragg peaks to lower angles had to be expected. To correct these shifts in the Rietveld program a polynomial $G(2\theta_K)$ of fifth degree was used to fit the results of the simulations. Finally the least-squares calculation was used to refine simultaneously any combination of the following parameters: lattice parameters a, b, c and β; Euler angles φ, θ and ψ; six background parameters; three parameters for the profiles; one asymmetry factor according to Wiles & Young (1981); orientation factor P; mean Grüneisen parameter $\bar{\gamma}$; scale offset δ and the intensity factor c of (2).

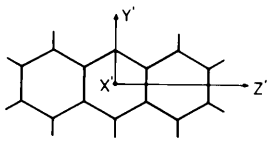

Fig. 2. The orthogonal $x'y'z'$ coordinate system of the anthracene molecule.

For the Rietveld program the unaltered input data consisted of the coordinates of the atoms and the translation and libration tensors for the temperature factor.

The pressure dependence of the lattice parameters is shown in Fig. 3. The data points are fitted by least squares to a polynomial of second order and it can be seen that the pressure dependence of lattice parameters is non-linear. As an example, the pressure dependence of the structure factor of the 001 reflection is shown in Fig. 4. The data points are fitted to a polynomial of second order and similarly a non-linear pressure dependence can be observed. Here and in Fig. 5 the solid circle is calculated from Mason's (1964) measurement at ambient pressure. In

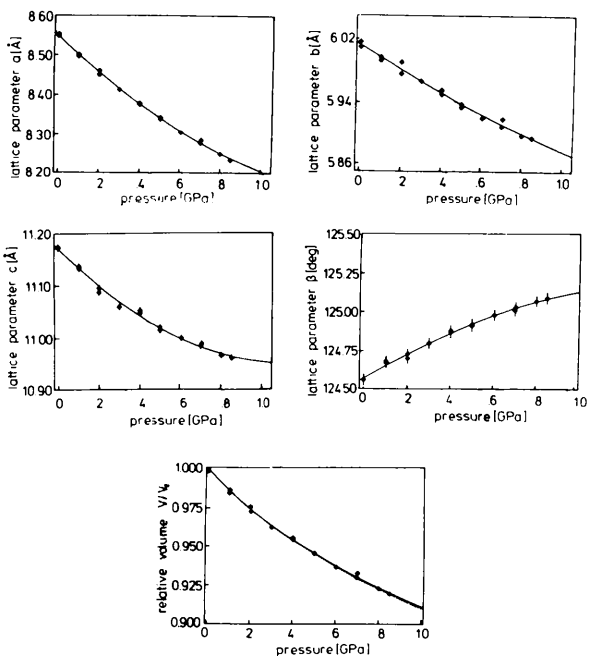

Fig. 3. The pressure dependence of the unit-cell parameters a, b, c, β and the relative unit-cell volume $V(p)/V(0)$. The pressure dependences are given by (p in GPa):
$a(p) = 8{\cdot}548\,(3) - 0{\cdot}484\,(17)p + 0{\cdot}141\,(14)p^2$;
$b(p) = 6{\cdot}012\,(3) - 0{\cdot}163\,(17)p + 0{\cdot}027\,(20)p^2$;
$c(p) = 11{\cdot}170\,(4) - 0{\cdot}388\,(20)p + 0{\cdot}171\,(24)p^2$;
$\beta(p) = 124{\cdot}56 + 0{\cdot}8491p - 0{\cdot}2654p^2$.

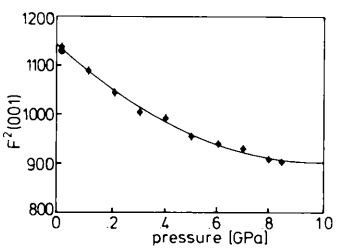

Fig. 4. The pressure dependence of the square of the structure factor $F(001)$. The approximation is given by $F^2(p) = 1132 - 455p + 234p^2$ (p in GPa).

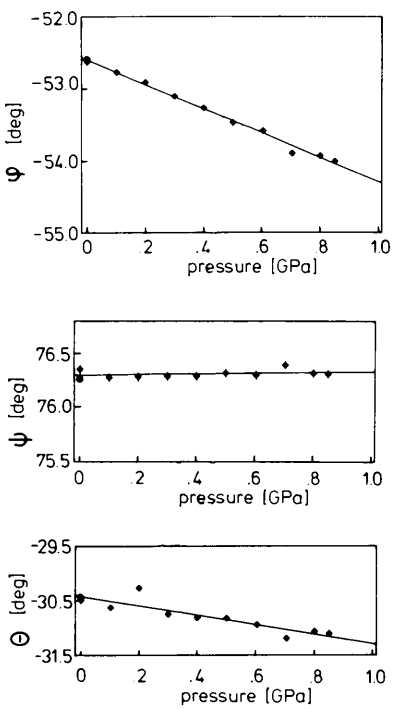

Fig. 5. The pressure dependence of the measured Euler angles: $\varphi = -52{\cdot}60\,(3) - 1{\cdot}69\,(5)p$; $\psi = 76{\cdot}29\,(2) + 0{\cdot}037\,(40)p$; $\theta = -30{\cdot}42\,(8) - 0{\cdot}86\,(16)p$ (p in GPa).

Table 1. *The angles (°) between the two orthonormal systems (x, y, z) and (x', y', z') at 0·0 GPa (left) and 0·85 GPa (right) (typical errors are 0·05°)*

	x	y	z		x	y	z
x'	36·03	115·31	66·17	x'	35·69	114·02	65·30
y'	71·37	26·38	72·01	y'	72·70	25·15	72·33
z'	119·60	96·93	30·56	z'	120·12	97·02	31·10

Table 2. *Williams's (upper part) and Kitaigorodski's (lower part) parameters as used in equation (7)*

Interaction	A (kJ mol^{-1} Å^{-6})	B (kJ mol^{-1})	α (Å^{-1})
H–H	114·3	11 112	3·74
H–C	523·3	36 701	3·67
C–C	2378·1	350 142	3·60
H–H	238·6	175 846	4·86
H–C	644·8	175 846	4·12
C–C	238·6	175 846	3·58

Fig. 5 results for the Euler angles are shown. The pressure dependence is linear and a straight line was fitted to the weighted data points. To see changes in orientation of the molecules under hydrostatic pressure, the angles between the orthonormal (x, y, z) system and the molecular (x', y', z') system are shown in Table 1 for pressures of 0 and 0·85 GPa respectively. The changes in magnitude are of the order of 1° or less.

IV. Model calculations

The lattice energy of molecular crystals can be described by atom-atom potentials. Every atom is considered to be the centre of a force interacting with all the other atoms of the neighbouring molecules. The lattice energy is supposed to be a superposition of such pair potentials. This model has been used successfully for a description of static and dynamic properties of molecular crystals. Especially for large anisotropic molecules the anisotropic shape and size of the molecular potentials is described quite well. The intermolecular interactions are based on semi-empirical atom-atom pair potentials,

$$U(r_{ij}) = B \exp(-\alpha r_{ij}) - A/r_{ij}^6, \qquad (6)$$

where r_{ij} is the distance between atoms i and j in different molecules. A, B and α depend on the type of ij interaction, C–C, C–H or H–H. The parameter values adopted are the Kitaigorodski (1966) and Williams (1967) parameters listed in Table 2. These parameters were obtained by fitting experimental data of organic molecular crystals (crystal structures, elastic constants and sublimation energies). Predictions about crystal structures can be made by a packing analysis of molecules, given that the total energy of a crystal must be a minimum.

The calculated pressure dependence of the normalized lattice parameters a, b and c are plotted in Fig. 6 for both parameter sets and compared with the measured values. For this calculation a method

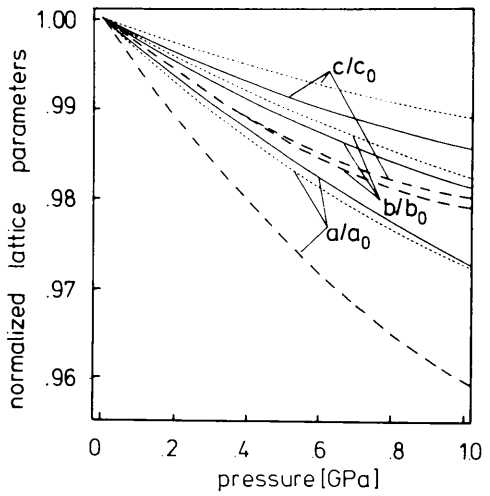

Fig. 6. The calculated relative unit-cell parameters a, b and c for Williams's (——) and Kitaigorodski's (· · ·) parameters and a comparison with measured relative unit-cell parameters (- - -).

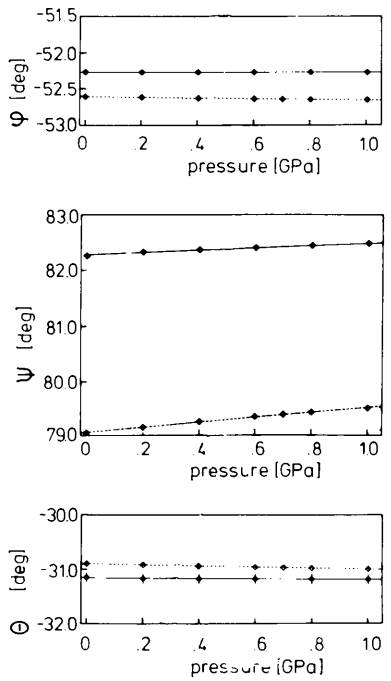

Fig. 7. The calculated pressure dependence of the Euler angles:
$\varphi_W = -52{\cdot}6117\,(5) - 0{\cdot}0469\,(7)p$;
$\varphi_K = -52{\cdot}2270\,(9) - 0{\cdot}014\,(14)p$;
$\psi_W = 79{\cdot}038\,(4) + 0{\cdot}446\,(6)p$;
$\psi_K = 82{\cdot}227\,(7) + 0{\cdot}217\,(12)p$;
$\theta_W = -30{\cdot}8967\,(4) - 0{\cdot}9026\,(7)p$;
$\theta_K = -31{\cdot}158\,(3) - 0{\cdot}035\,(5)p$.
The indexes W and K stand for Williams's (· · ·) and Kitaigorodski's (——) parameters respectively.

Table 3. *Measured and calculated unit-cell parameters of anthracene*

For the calculations Williams's (*W*) and Kitaigorodski's (*K*) potential parameters were used.

T (K)	*a* (Å)	*b* (Å)	*c* (Å)	*β* (°)	References
290	8·562 (6)	6·038 (8)	11·184 (8)	124·71 (10)	Mason (1964)
293	8·561 (10)	6·035 (10)	11·165 (10)	124·71 (17)	Kozhin & Kitaigorodski (1953)
296	8·543 (5)	6·002 (5)	11·164 (5)	124·62 (10)	Bokhenkov *et al.* (1986)
298	8·542 (5)	6·016 (6)	11·163 (5)	124·59 (7)	Lehmann & Pawley (1972)
300	8·561 (10)	6·036 (10)	11·163 (10)	124·71 (7)	Mathieson, Robertson & Sinclair (1950)
300	8·550 (8)	6·028 (8)	11·172 (8)	124·58 (8)	Ryzhenkov & Kozhin (1967)
293	8·553 (5)	6·016 (4)	11·172 (6)	124·56 (4)	This work
4·7	8·378 (4)	5·981 (4)	11·059 (5)	125·43 (10)	Bokhenkov *et al.* (1986)
0	7·971 (2)	6·242 (2)	10·947 (2)	123·86 (1)	This work (*K*)*
0	8·276 (2)	5·932 (2)	11·006 (2)	124·39 (1)	This work (*W*)*

* Calculated values.

described by Pawley & Mika (1974) was used. Between 0 and 0·85 GPa the calculated change of the angle β amounts to 0·02°. This has to be compared with a measured change of 0·53° in this pressure range (see Fig. 3). The calculated Euler angles (see Fig. 7) are adequately represented by linear functions.

V. Discussion

In Table 3 some published lattice parameters are shown for room temperature at normal pressure. Calculated atom-atom-potential results are marked with an asterisk and the consistency of our measured lattice parameters with the literature is good. The calculated angle β seems to be too small and shows a deficiency of the model. Such a smaller angle β has been already found by Alt & Kalus (1982) for naphthalene.

Lattice parameters from calculations correspond to $T = 0$ K. We would expect that measured lattice parameters decrease at lower temperatures. With the exception of *b* calculated by the parameter set of Kitaigorodski, the other calculated unit-cell parameters *a*, *b* and *c* are systematically slightly lower than the measured values at 300 K. If we compare absolute values, the Williams parameter set yields better results for anthracene. It is also found that the measured 4·7 K values of Bokhenkov, Kolesnikov, Maier & Fedotov (1986) are close to those calculated with the Williams parameter set.

If we compare the relative lattice parameters at different pressures (Fig. 6), the anisotropy for different crystal directions can be clearly seen. It is also observed that the crystal becomes stiffer if we apply pressure and this is a well known result. The calculated changes of the relative lattice parameters are always distinctly smaller than those of the measured values. To select the best parameter set it would be necessary to make measurements at $T = 0$ K or to apply corrections using at least a temperature-dependent bulk modulus. A calculation at ambient temperature has to incorporate anharmonic interactions, and is quite complicated. Some attempts are discussed in the literature (see, for example, Jindal & Kalus, 1986), taking into account higher-order perturbation theory. Unfortunately there are no good pressure-dependent data of the unit-cell parameters available for anthracene at low temperatures. However, Häfner & Kiefer (1987) proposed an extrapolation scheme for the pressure and temperature dependence of the unit-cell volume *V*, using mainly high-pressure data at room temperature. The following equations for anthracene were used:

$$(V/V_0)^C = \frac{(B_1 - C)(p_0 + p) + 2B_0}{(B_1 + C)(p_0 + p) + 2B_0} \tag{7}$$

where

$$p_0 = \frac{2B_0\{1 - [V(T)/V(300)]^C\}}{(B_1 + C)[V(T)/V(300)]^C - (B_1 - C)} \tag{8}$$

and $C^2 = B_1^2 - 2B_2B_0$, $B_0 = 6{\cdot}786$ GPa, $B_1 = 8{\cdot}960$, $B_2 = -0{\cdot}926$ GPa^{-1}, $V(T)$ and $V(300) = V_0$ are the unit-cell volumes at temperatures *T* and 300 K respectively and at pressure $p = 0$. A graphical representation of the pressure and temperature dependence of the volume of anthracene is given in the paper mentioned above. Using these equations we can calculate the pressure dependence of *V* at 300 and 0 K and find that $V(0)/V(300) = 0{\cdot}962$:

$$W = \left|\frac{\mathrm{d}V(300)/\mathrm{d}p}{\mathrm{d}V(0)/\mathrm{d}p}\right|_{p\to 0} = \frac{[(B_1 + C)p_0 + 2B_0]^{(1/C+1)}}{4[(B_1 - C)p_0 + 2B_0]^{(1/C-1)}B_0^2} = 1{\cdot}61$$

where $p_0 = 0{\cdot}416$ GPa for $T = 0$.

This means that the isothermal compressibility $\kappa = -(\partial V/\partial p)_T/V$ at 0 K is about 1·61 lower than at 300 K. We can therefore now assume that the following relations hold approximately for $p \to 0$:

$$(\mathrm{d}a/\mathrm{d}p)^*_{T=300\,\mathrm{K}} = W(\mathrm{d}a/\mathrm{d}p)_{T=0};$$

$$(\mathrm{d}b/\mathrm{d}p)^*_{T=300\,\mathrm{K}} = W(\mathrm{d}b/\mathrm{d}p)_{T=0}$$

and

$$(\mathrm{d}c/\mathrm{d}p)^*_{T=300\,\mathrm{K}} = W(\mathrm{d}a/\mathrm{d}p)_{T=0}$$

Table 4. *The slopes of the normalized lattice parameters*

The first two rows are experimental results, the last two are calculated values. Units are GPa^{-1}.

$-(da/dp)/a$	$-(db/dp)/b$	$-(dc/dp)/c$	Comments
0·058	0·027	0·035	Experimental data 300 K
0·036	0·017	0·022	Extrapolated data 0 K
0·033	0·025	0·020	Williams parameter
0·035	0·023	0·015	Kitaigorodski parameter

with $W = 1{\cdot}61$. The asterisk means 'measured values', whereas the right-hand side means 'calculated values at 0 K'. Surprisingly, it is found that this correction of measured values reproduces the calculated slopes of the normalized lattice parameters quite reasonably (see Table 4). But on the basis of these experimental results we cannot find a clear decision in favour of one of the two parameter sets. We have to mention here that the lattice constants (see Table 3) seem to favour the Williams set of parameters.

To explain the pressure dependence of the structure factor, different aspects must be considered. For example, some reflection intensities increase while others decrease in intensity when pressure is applied. Under pressure, the reflections are shifted to higher scattering angles. In this case the atom form factor and the Debye-Waller factor decrease. Under pressure, however, the amplitudes of the oscillating atoms become smaller and the drop in magnitude of the Debye-Waller factor is therefore reduced. The change of the phases with pressure occurs in both directions. Depending on these effects, the structure factor can increase, remain constant or decrease with pressure.

The Euler angles display only a linear pressure dependence within the pressure range of the present experiment. If we compare this with the calculated Euler angles the dependence is the same, but neither the sign nor the magnitude of the pressure dependences are reproduced correctly by the calculations. This discrepancy is especially large for the Euler angle φ whereas the slopes of ψ and θ nevertheless remain small. It seems to us that the crystal structure depends to some extend on electrostatic long-range interactions, as already discussed by Murthy, O'Shea & McDonald (1983). Such interactions are not taken into account in our model calculations.

References

ALT, H. & KALUS, J. (1982). *Acta Cryst.* B**38**, 2595-2600.

BLOCH, D., PAUREAU, J., VOIRON, J. & PARISOT, G. (1976). *Rev. Sci. Instrum.* **47**, 296-298.

BOKHENKOV, E. L., KOLESNIKOV, A. I., MAIER, I. & FEDOTOV, V. G. (1986). Private communication.

CRUICKSHANK, D. W. J. (1956). *Acta Cryst.* **9**, 915-923.

DORNER, B., BOKHENKOV, E. L., CHAPLOT, S. L., KALUS, J., NATKANIEC, I., PAWLEY, G. S., SCHMELZER, U. & SHEKA, E. F. (1982). *J. Phys. C*, **15**, 2353-2365.

HÄFNER, W. & KIEFER, W. (1987). *J. Chem. Phys.* **86**, 4582-4596.

JINDAL, V. K. & KALUS, J. (1986). *Phys. Status Solidi B*, **133**, 89-99.

KITAIGORODSKI, A. I. (1966). *J. Chim. Phys. Phys. Chim. Biol.* **63**, 9-16.

KOZHIN, V. M. & KITAIGORODSKI, A. I. (1953). *Zh. Fiz. Kim.* **27**, 1676-1681.

LEHMANN, M. S. & PAWLEY, G. S. (1972). *Acta Chim. Scand.* **26**, 1996-2004.

MASON, R. (1964). *Acta Cryst.* **17**, 547-555.

MATHIESON, A. MCL., ROBERTSON, J. M. & SINCLAIR, V. C. (1950). *Acta Cryst.* **3**, 245-250.

MURTHY, C. S., O'SHEA, S. F. & MCDONALD, I. R. (1983). *Mol. Phys.* **50**, 531-541.

PAWLEY, G. S. (1967). *Phys. Status Solidi*, **20**, 347-360.

PAWLEY, G. S. & MIKA, K. (1974). *Phys. Status Solidi B*, **66**, 679-686.

RIETVELD, H. M. (1967). *Acta Cryst.* **22**, 151-152.

RYZHENKOV, A. I. & KOZHIN, V. M. (1967). *Kristallografiya*, **12**, 1079-1086.

SCHMELZER, U., BOKHENKOV, E. L., DORNER, B., KALUS, J., MACKENZIE, G. A., NATKANIEC, I., PAWLEY, G. S. & SHEKA, E. F. (1981). *J. Phys. C*, **14**, 1025-1041.

WILES, D. B. & YOUNG, R. A. (1981). *J. Appl. Cryst.* **14**, 149-151

WILLIAMS, D. E. (1967). *J. Chem. Phys.* **47**, 4680-4684.

Acta Cryst. (1988). A**44**, 1065-1072

Quantitative Determination of Phases of X-ray Reflections from Three-Beam Diffraction. I. Theoretical Considerations

BY SHIH-LIN CHANG AND MAU-TSU TANG

Department of Physics, National Tsing Hua University, Hsinchu, Taiwan 30043

(*Received* 22 *March* 1988; *accepted* 22 *June* 1988)

Dedicated to Professor Dr Ulrich Bonse on the occasion of his 60th birthday

Abstract

A method of quantitative determination of X-ray reflection phases using three-beam multiple diffraction is described. This method is derived from the dynamical theory of X-ray diffraction. First-order approximation is employed to take care of the multibeam diffraction situation. Polarization and excitation of wave fields and the Lorentz factor of crystal rotation are considered. For practical purposes,

0108-7673/88/061065-08$03.00